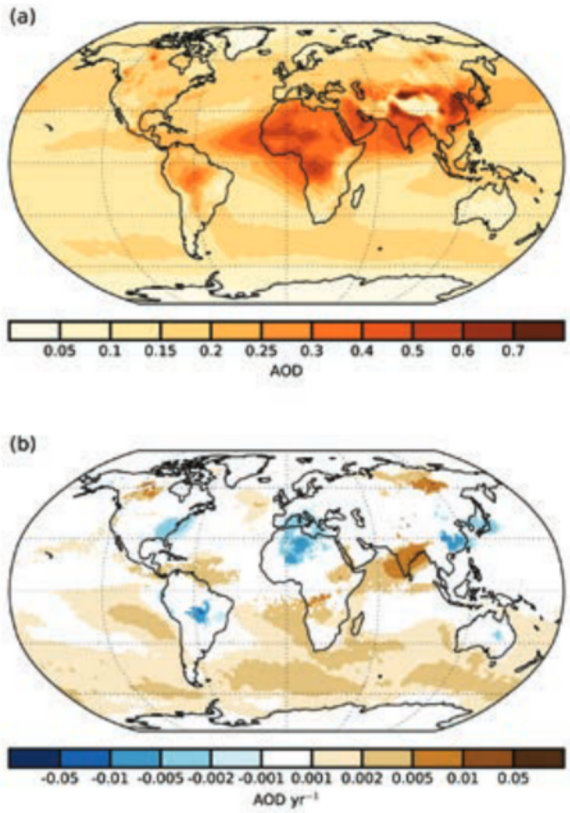

Fig. 2.50. (a) Total 550-nm AOD averages for 2003–17. Note the regional differences, with much greater total AOD values over parts of northern Africa, the Arabian Peninsula, southern Asia, and eastern China. (b) Linear trends of total AOD (AOD yr^{-1}) for 2003–17. Only trends that are statistically significant (95% confidence) are shown.

strong year in terms of aerosol radiative forcing, with the third consecutive increase in RFari, estimated to be −0.68 W m^{-2} in 2017, stronger than the −0.55 W m^{-2} estimated for 2015. The increase may be linked to increased biomass-burning aerosols in the tropics. Trends remain statistically fragile, however, because of large uncertainties in the estimates. Absorbing anthropogenic aerosols exert positive RFari over bright surfaces, like the African and Arabian deserts, as shown in the upper panel of Fig. 2.51. RFaci, estimated at −0.8 W m^{-2} in 2017, was comparable to 2015 (−0.82 W m^{-2}) and 2016 (−0.77 W m^{-2}).

4) Stratospheric ozone—M. Weber, W. Steinbrecht, R. van der A, S. M. Frith, J. Anderson, M. Coldewey-Egbers, S. Davis, D. Degenstein, V. E. Fioletov, L. Froidevaux, D. Hubert, J. de Laat, C. S. Long, D. Loyola, V. Sofieva, K. Tourpali, C. Roth, R. Wang, and J. D. Wild

Throughout nearly the entire Southern Hemisphere annual mean total column ozone levels in 2017 were above the mean from the 1998–2008 reference period (Plate 2.1y). In particular, the Antarctic region showed values that were more than 10 DU (Dobson units) above the long-term mean (see also October mean in Fig. 2.52e). The main cause was the weak polar vortex (stratospheric cyclone) observed in southern winter/spring resulting in below-average polar ozone losses and a rather small ozone hole in size and depth (see Section 6h). In the second half of 2017 the quasi-biennial oscillation (QBO) was in the east phase (easterly flow in the tropical lower stratosphere), which had a global impact on the stratospheric circulation. During the QBO east phase planetary waves are deflected toward the pole (SH winter in 2017) and weaken the polar vortex (Baldwin et al. 2011). Associated with these planetary waves is an enhanced meridional or Brewer–Dobson circulation transporting more ozone into middle to high latitudes which, in addition to reduced polar losses, contributed to the overall SH increase (e.g., Salby 2008; Weber et al. 2011). In the Northern Hemisphere total ozone was generally near

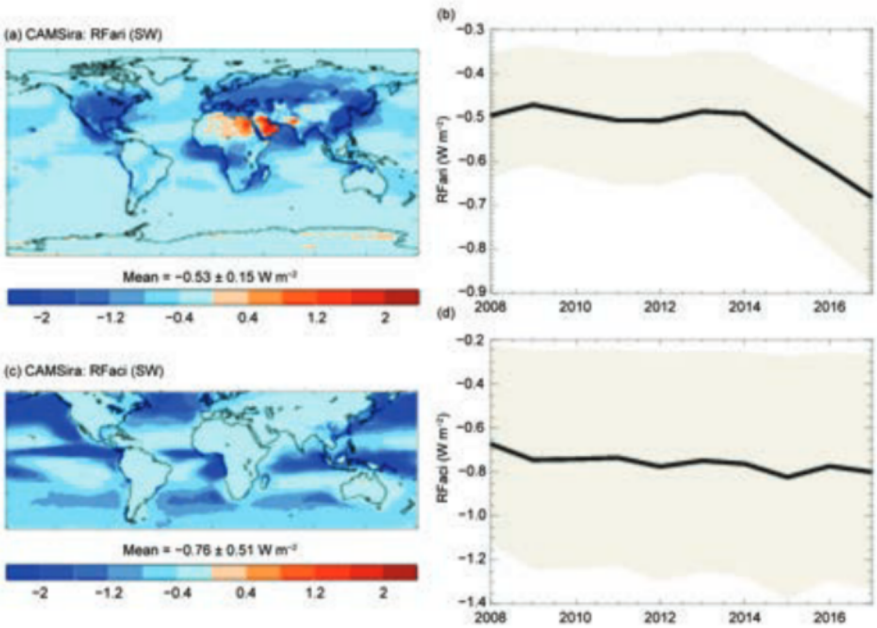

Fig. 2.51. Radiative forcing (W m^{-2}) in the SW spectrum resulting from (a) RFari and (c) RFaci from 2008–17. (b,d) The uncertainties of these estimates are shown in gray.

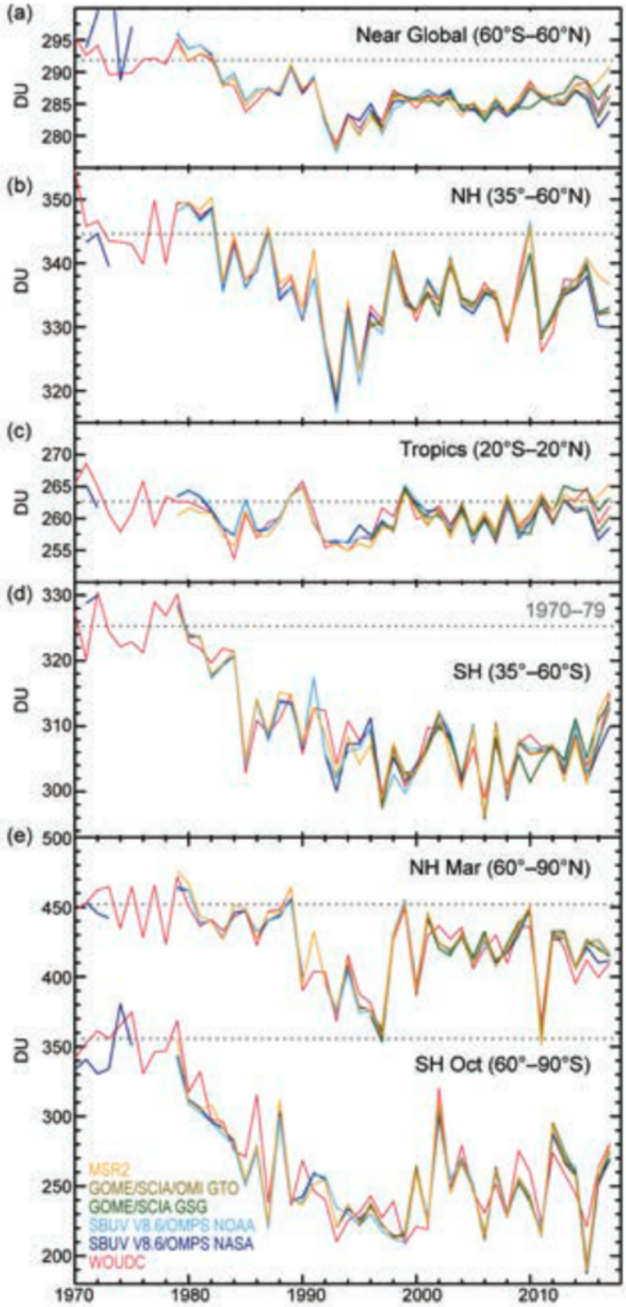

Fig. 2.52. Time series of annual mean total ozone (DU) in (a)–(d) four zonal bands, and (e) polar (60°–90°) total ozone in Mar (NH; see also Section 5j) and Oct (SH), the months when polar ozone losses usually are largest. Data are from WOUDC (World Ozone and Ultraviolet Radiation Data Centre) ground-based measurements combining Brewer, Dobson, SAOZ, and filter spectrometer data (Fioletov et al. 2002, 2008); the BUV/SBUV/SBUV2 V8.6/OMPS merged products from NASA (MOD V8.6, Frith et al. 2014, 2017) and NOAA (Wild and Long 2018, manuscript in preparation); the GOME/SCIAMACHY/GOME-2 products from University of Bremen (Weber et al. 2011; Weatherhead et al. 2017) and GTO from ESA/DLR (Coldewey-Egbers et al. 2015; Garane et al. 2018). MSR-2 assimilates nearly all ozone datasets after corrections with respect to the ground data (van der A et al. 2015). All six datasets have been bias corrected by subtracting averages from the reference period 1998–2008 and adding the multiple data mean from the same period. The horizontal dotted gray lines in each panel show the average ozone level for 1970–79 calculated from the WOUDC data. All data from 2017 are preliminary.

average in 2017 with some regions with slightly lower ozone (Plate 2.1y).

Figure 2.52 shows the annual mean total ozone time series from various merged datasets in the tropics, extratropics, and selected months in the polar regions as well as the near-global (60°N–60°S) average. For all time series, the average ozone levels from the 1970s, a time when ozone losses due to ozone-depleting substances were still very small, are also shown. Except for the tropics, total ozone levels have not yet recovered to the values from the 1970s. A recent study indicates that total ozone trends since the late 1990s are positive (<1% decade^{-1}) but only reach statistical significance at a few latitudes (Weber et al. 2018). The small increase in global total ozone following the significant decline before the 1990s is regarded as proof that the Montreal Protocol and its Amendments, signed thirty years ago and responsible for phasing out ozone-depleting substances (ODS), works.

ODS currently decrease at about one-third of the absolute increasing rate before the 1990s, but the recent increase in total column ozone is in comparison smaller than expected from the ODS change. Model studies show that the predicted ozone evolution is consistent in most regions outside the tropics with ODS changes and observed stratospheric ozone and total column observations (Shepherd et al. 2014; Chipperfield et al. 2017). The lack of observed ODS-related changes in tropical total ozone (but observed in climate models with stratospheric chemistry) may be due to a compensation by increases in tropospheric ozone that contribute to the total column (Shepherd et al. 2014). However, observed global tropospheric ozone trends from various studies are highly variable and often insignificant (Gaudel et al. 2018 and Figure 26 therein).

Ball et al. (2018) suggest, based on an analysis of satellite measurements, that a near-continuous, near-global (< 60° in both hemispheres) decline in lower stratospheric ozone since 1998 was compensated by observed upper stratospheric increases and tropospheric increases, resulting in rather small total ozone trends. A recent chemistry-transport model study by Chipperfield et al. (2018) shows that the observed

lower stratospheric and total column ozone changes are mostly explained by variability in atmospheric dynamics and is not contradicting our current understanding of stratospheric ozone chemistry related to ODS changes as otherwise suggested by Ball et al. (2018). In the tropics a continuous decline in total ozone in the future is predicted by chemistry-climate models as climate change will enhance tropical upwelling and potentially thin ozone in the lowermost tropical stratosphere, thus increasing UV radiation in the equatorial region (WMO 2014; Chipperfield et al. 2017).

While the expected slow recovery of stratospheric ozone has not yet resulted in substantial increases of total column ozone, ozone in the upper stratosphere has been showing clearer signs of increase and recovery over the last 10 to 15 years (WMO 2014; Steinbrecht et al. 2017). Figure 2.53 shows that since about 2000, ozone has generally been increasing in the upper stratosphere, ending the previous period of ozone decline. In 2017, ozone values in the upper stratosphere were below the EESC curve both in the tropical belt and at northern midlatitudes. This is somewhat surprising for the easterly phase of the QBO and may in part arise from the decadal

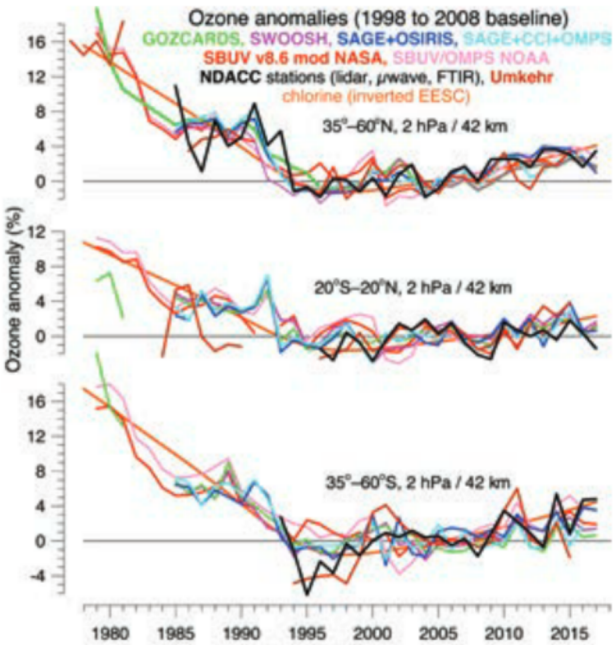

Fig. 2.53. Annual mean anomalies of ozone (%; 1998–2008 baseline) in the upper stratosphere, near 42-km altitude or 2-hPa pressure for three zonal bands: 35°–60°N (NH), 20°N–20°S (tropics), and 35°–60°S (SH). Colored lines are for long-term records obtained by merging different limb (GOZCARDS, SWOOSH, SAGE+OSIRIS, SAGE+CCI+OMPS-LP) or nadir viewing (SBUV, OMPS-NP) satellite instruments. Black line is from merging ground-based ozone records at NDACC stations employing differential absorption lidars, microwave radiometers, and/or Fourier Transform InfraRed spectrometers (FTIRs). Gray line is for ground-based Umkehr measurements. See Steinbrecht et al. (2017) for details on the various datasets. Orange line gives inverted EESC as a proxy for man-made ozone depletion. Ozone data for 2017 are not yet complete for all instruments and are still preliminary.

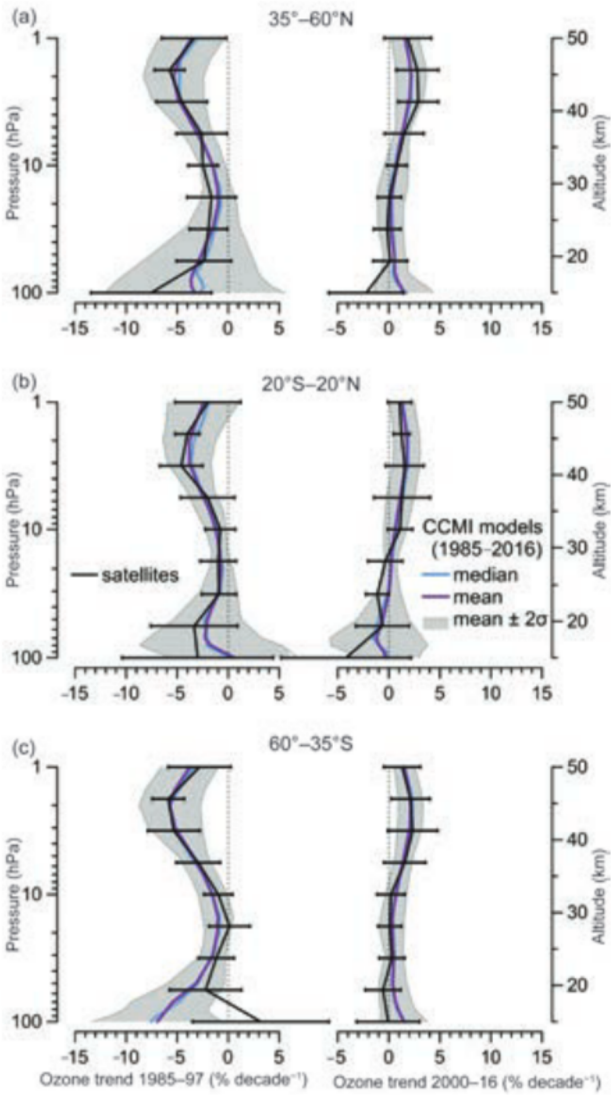

Fig. 2.54. Mean ozone trends in the upper atmosphere (% decade^{-1}) prior to 1997 and after 2000 as derived from the CCMI REF-C2 models' simulation (median in blue and mean in purple) and satellite data (black line) in three zonal bands: (a) 35°–60°N (NH), (b) 20°N–20°S (tropics), and (c) 35°–60°S (SH). Mean trends were averaged from trends of individual model runs and various merged datasets shown in Fig. 2.53. The shading shows the 2σ of the models' mean trend. Same type of multilinear regression analysis was used to determine the trends in models and observations. Adapted from LOTUS (2018, SPARC report under review).

minimum of solar activity (e.g., Randel and Wu 1996; Newchurch et al. 2003; WMO 2014).

It is a challenge to accurately attribute observed stratospheric ozone changes, because changes due to recovery are expected to be small and thus potentially masked by long-term natural variability and measurement uncertainty. Substantial efforts, therefore, have gone into improving the available observational ozone profile records and into better ways to estimate ozone profile trends and their uncertainties (LOTUS 2018, *SPARC report* under review). Figure 2.54 shows the resulting updated trend profiles from observations and chemistry-climate models, both during the phase of ODS-driven ozone decline from the late 1970s to the late 1990s, and during the beginning recovery phase from 2000 to 2016. Observations are in generally good agreement with chemistry–climate model simulations.

As a result of the Montreal Protocol and its Amendments, ODS have been declining in the stratosphere since the late 1990s. The model simulations predict that ozone in the upper stratosphere should now increase by 2%–3% decade^{-1}, due to both declining ODS and stratospheric cooling, the latter caused by increasing greenhouse gases (WMO 2014). The right panels of Fig. 2.54 demonstrate that ozone increases are observed in the upper atmosphere after 2000, although they are not statistically significant at all latitudes and altitudes. Nevertheless, the good agreement between model simulations and observations gives confidence that ozone trends in the upper stratosphere are well understood and that ozone in that region is on its continuing (slow) path towards recovery.

5) Stratospheric water vapor—S. M. Davis, K. H. Rosenlof, D. F. Hurst, H. B. Selkirk, and H. Vömel

Stratospheric water vapor (SWV) is a radiatively important gas that can also impact stratospheric ozone chemistry. The second consecutive year of dramatic changes in lower SWV occurred in 2017. Following 2016, during which the tropical mean (15°N–15°S) water vapor anomaly in the lowermost stratosphere (at 82 hPa) dropped from a near record high in January (+0.5 ppm, parts per million mole fraction, equivalent to μmol mol^{-1}) to a record low by December (–1 ppm), 2017 anomalies increased to near record high values by midyear.

In January 2017 negative (dry) anomalies were observed in the tropics and subtropics, in stark contrast to the strong positive (wet) anomalies of June 2017. From January to June 2017, the tropical SWV anomaly in the lower stratosphere increased by 0.9 ppm (Figs. 2.55, 2.56c,d), about 40% of the average seasonal cycle amplitude at 82 hPa in the tropics and 140% of the climatological average difference between these two months. This steep increase in tropical lowermost SWV during the first half of 2017 and subsequent return to near-normal values by the end of the year were observed by both the *Aura* Microwave Limb Sounder (MLS) satellite instrument (Fig. 2.55) and balloon-borne frost point hygrometer soundings at tropical sites Hilo, Hawaii (20°N), and San José, Costa Rica (10°N) (Figs. 2.56c,d).

Variations in cold-point temperatures (CPTs) in the tropical tropopause layer (TTL) on annual and interannual timescales provide the dominant control on water vapor entering into the lowermost stratosphere in the tropics by freeze-drying tropospheric air during its slow ascent through the TTL. Thus, seasonal to interannual variability in tropical SWV around 82 hPa is highly correlated with CPT variations. The dramatic swing in tropical lower SWV during 2017 is consistent with the substantial 2.5°C increase from November 2016 to May 2017 and subsequent 1.5°C decrease in tropical CPT anomalies over the remainder of 2017 (Fig. 2.56d).

Interannual variations in CPTs are partially related to interannual variability in the phases of ENSO

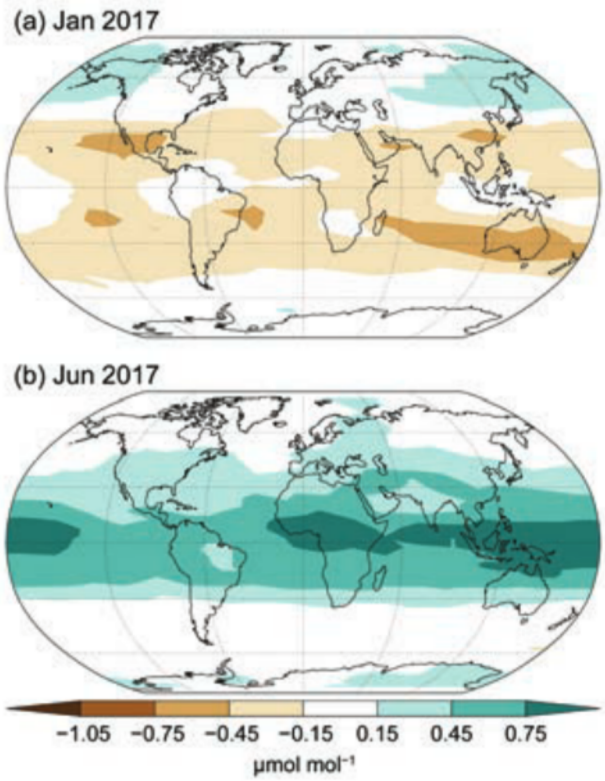

Fig. 2.55. Global stratospheric water vapor anomalies (μmol mol^{-1}; 2004–17 base period) centered on 82 hPa in (a) Jan and (b) Jun 2017 from the *Aura* MLS.